PHILOSOPHICAL TRANSACTIONS OF THE ROYAL SOCIETY A MATHEMATICAL, PHYSICAL & ENGINEERING SCIENCES

Experimental Tests of Quantum Chromodynamics

D. H. Perkins

Phil. Trans. R. Soc. Lond. A 1982 **304**, 23-41
doi: 10.1098/rsta.1982.0003

Phil. Trans. R. Soc. Lond. A **304**, 23–41 (1982) [23]
Printed in Great Britain

Experimental tests of quantum chromodynamics

By D. H. Perkins, F.R.S.
Nuclear Physics Laboratory, University of Oxford, Keble Road, Oxford OX1 3RH, U.K.

Experimental results from deep inelastic lepton–nucleon scattering, from electron–positron annihilation to hadrons and from massive lepton-pair production in hadron collisions, are discussed. The data obtained so far give qualitative support for QCD. Serious quantitative comparisons are beset with difficulties, which arise first because of discrepancies between different experiments, and secondly because in addition to the perturbative effects that have been calculated theoretically, there are non-perturbative contributions for which there are no reliable estimates. These appear to be important in the momentum transfer range that can be investigated experimentally at present.

1. Introduction

Quantum chromodynamics (QCD) is the renormalizable, non-Abelian gauge theory of inter-quark forces. Some, but not all, of the essential components of this model are well established. First, *quark substructure* provides the only satisfactory description of the heavy meson states $\psi, \psi', \Upsilon'', \ldots, \Upsilon, \Upsilon', \Upsilon'', \ldots$ in the 3–4 GeV and 9.5–10.5 GeV mass regions. Comparison of charmonium states with those of positronium shows a striking similarity (figure 1), and one concludes that $\psi, \psi', \ldots$ consist of particle–antiparticle bound states, $c\bar{c}$, of heavy quarks in a potential not too far from the coulomb form. Some information about the interquark potential is obtained from the $2\,^3S_1$–$1\,^3S_1$ separation in charmonium, $\Delta E_\psi = (M_{\psi'} - M_\psi)\,c^2 = 589$ MeV, as compared with that in the upsilon system, $\Delta E_\Upsilon = (M_{\Upsilon'} - M_\Upsilon)\,c^2 = 560$ MeV. For a pure Coulomb potential, $\Delta E \propto \mu$, the quark mass, while for a potential rising as kr, $\Delta E \propto \mu^{-\frac{1}{3}}$. For the combination of coulomb and confining term

$$V = -\tfrac{4}{3}\alpha_s/r + kr, \tag{1}$$

the two values of ΔE can be made equal by choice of α_s. We set $k = 0.2$ GeV^2 from the string model, and the slope of Regge trajectories $\alpha' = (2\pi k\hbar c)^{-1} = 0.9$ GeV^{-2}, and thus obtain for the 'strong coupling constant', $\alpha_s \approx 0.40$.

So, a colour field carried by massless gluons of coulombic form at small r fits the bound states. The existence of the colour degree of freedom is necessitated by the value of $R = \sigma(e^+e^- \to \text{hadrons})/\sigma(e^+e^- \to \mu^+\mu^-)$ for $10 < E_{c.m.} < 35$ GeV, as indicated in figure 2. Over this range R is constant, and compatible with the value $\frac{11}{3}$ expected for u, d, s, c and b quarks in $N_c = 3$ colours. The rate for $\pi^\circ \to 2\gamma$, via a u, d quark loop, is proportional to $N_c^2(Q_u^2 - Q_d^2)^2$; the observed lifetime gives $N_c = 2.98 \pm 0.11$.

The colour force is assumed to be carried by an octet of colour–anticolour massless vector gluons. A characteristic feature of this octet structure and the colour singlet nature of baryons and mesons is that the hyperfine splitting, $m_\rho - m_\pi \approx 600$ MeV, is predicted to be just twice that for baryons, $m_\Delta - m_N \approx 300$ MeV. Finally, the narrowness of the bound states $\psi, \Upsilon, \ldots$ can perhaps be understood in the colour model. Since a colour singlet of $c\bar{c}$ or $b\bar{b}$ quarks, of C-parity $= -1$ (since they couple to photons), must transform to a colour singlet of pions, an

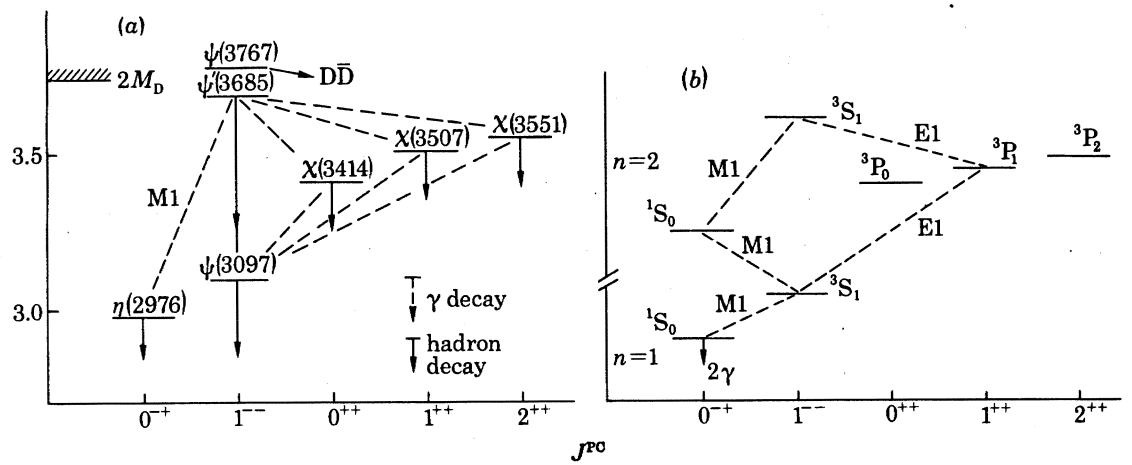

FIGURE 1. Energy levels of (*a*) charmonium and (*b*) positronium.

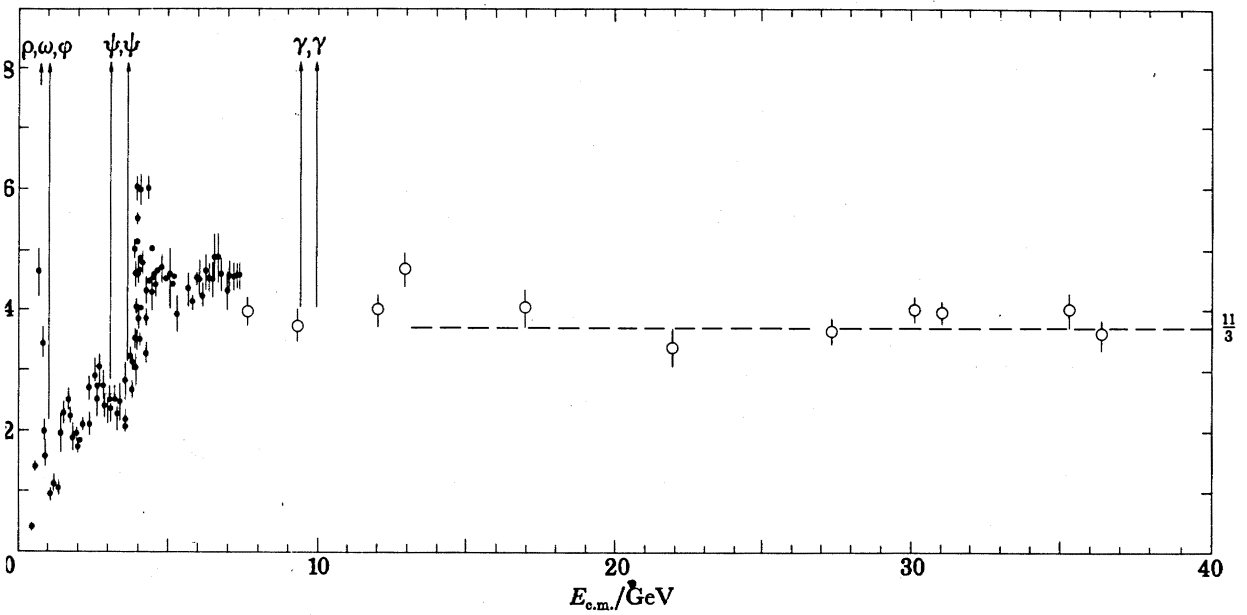

FIGURE 2. Value of $R = \sigma(e^+e^- \to \text{hadrons})/\sigma(e^+e^- \to \mu^+\eta^-)$, as measured in various experiments. For $E > 10$ GeV, all the data are from the PETRA storage ring at DESY.

odd number of gluons is involved and three-gluon exchange is the simplest possibility. For a vector meson such as ψ

$$\Gamma(\psi \to e^+e^-) = (16\pi\alpha^2/M^2)\,|\psi(0)|^2\,(\Sigma C_i Q_i)^2 = 5\ \text{keV}, \tag{2}$$

while for hadronic decay

$$\Gamma(\psi \to 3G) = \tfrac{160}{81}\{(\pi^2-9)\,\alpha_s^3/M^2\}\,|\psi(0)|^2 = 70\ \text{keV} \tag{3}$$

requiring however a smaller number, $\alpha_s \approx 0.20$, than the potential (1).

PHILOSOPHICAL TRANSACTIONS OF THE ROYAL SOCIETY A MATHEMATICAL, PHYSICAL & ENGINEERING SCIENCES

2. Crucial quantitative tests of QCD

The observations of the ψ, Υ, ... bound states of $Q\bar{Q}$, while qualitatively what we expect of QCD, are not very quantitative because:

(*a*) QCD effects can only be calculated with confidence from perturbation theory, requiring α_s small (cf. the value 0.4 from the ψ-levels).

(*b*) The characteristic feature of QCD is the non-Abelian nature of the coupling, which requires α_s to decrease slowly with increasing q^2, for which a much larger dynamic range in q^2 is needed for a significant test.

So, the crucial first equations to be answered are

(*a*) Does the running coupling constant α_s actually run?

(*b*) Is there a strong gluon–gluon coupling?

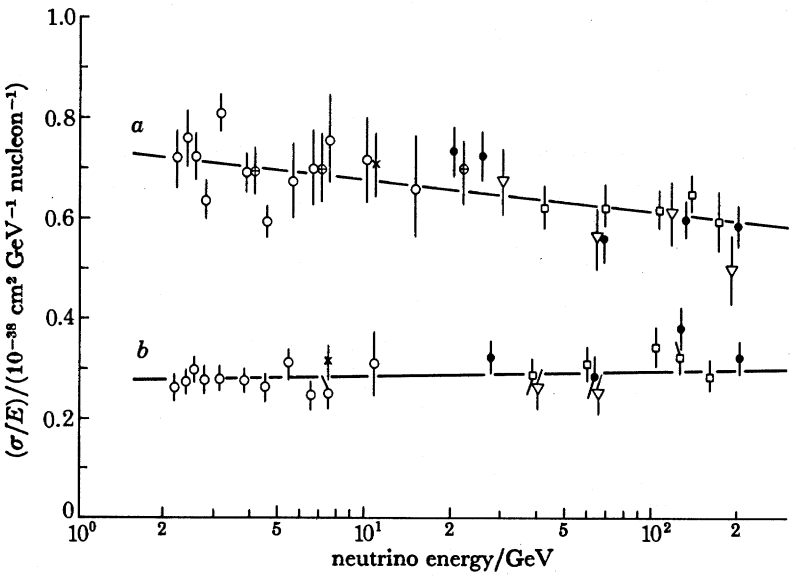

Figure 3. Neutrino (*a*) and antineutrino (*b*) total cross sections on nucleons, divided by the incident energy. The data come from a variety of bubble chamber and counter experiments at Fermilab, Cern and Serpukhov.

3. Deep inelastic lepton hadron scattering

Data on deep inelastic scattering of leptons (electrons, muons, neutrinos) by nucleons have been accumulated for over a decade, and now cover the range $0.1 \leqslant q^2 \leqslant 150\ \mathrm{GeV}^2$ with quoted levels of accuracy on the structure functions $F(x, q^2)$ of 10% or better. However, we still have far from a comprehensive picture. Data from different experiments disagree. For a given set of data, different methods of analysis reach different conclusions. I hope I shall not add to the confusion.

3.1. *The parton model*

The first point to remember is that the parton model is very good. Neutrino cross sections (figure 3) are nearly proportional to energy. The constituent partons *are* nearly point-like and nearly free, and they can be identified with quarks. First, they have spin-$\frac{1}{2}$ because:

(i) The ratio $2xF_1/F_2$ in the SLAC e–d experiments (figure 4) is unity as expected from the Callan–Gross relation (1969) for spin-$\frac{1}{2}$ partons in the limit of large q^2.

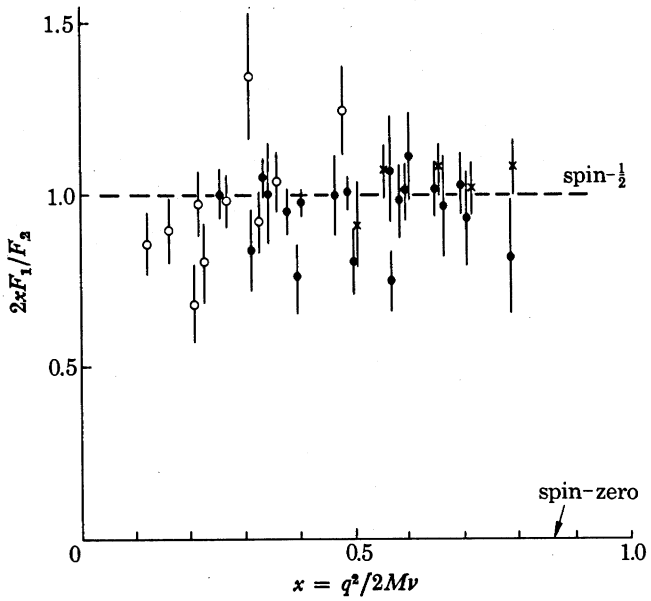

FIGURE 4. The ratio of magnetic to electric scattering, $2xF_1/F_2$ from SLAC experiments (Riordan *et al.* 1975). For spin-$\frac{1}{2}$ constituents, a ratio of unity is expected in the limit $q^2 \to \infty$: ϕ, $1.5 < q^2 < 4$ GeV²; ●, $5 < q^2 < 11$ GeV²; ×, $12 < q^2 < 16$ GeV².

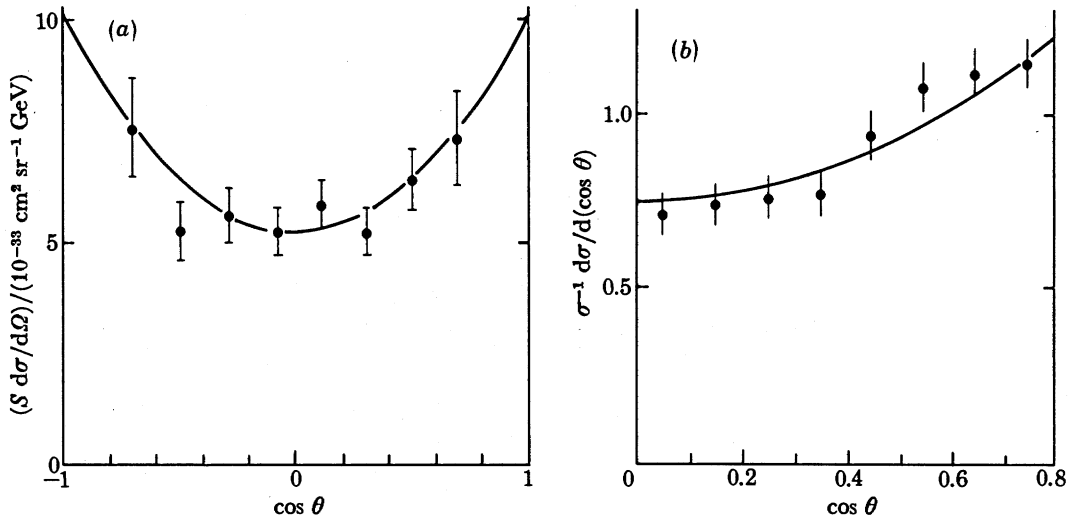

FIGURE 5. The angular distribution, relative to the beam axis, for the processes (*a*) $e^+e^- \to \mu^+\mu^-$ and (*b*) e^+e^- → two hadron jets ($27 < W < 37$ GeV) (after Wiik 1980).

(ii) The angular distribution of 'two-jet' events in e^+e^- annihilation at $25 < W < 35$ GeV has the characteristic $(1+\cos^2\theta)$-distribution expected for spin-$\frac{1}{2}$–spin-$\frac{1}{2}$ scattering, just like $e^+e^- \to \mu^+\mu^-$. (figure 5).

(iii) In the Drell–Yan process of dilepton production in hadron collisions, viewed as fusion of a quark from the projectile with an antiquark from the target, the angular distribution of muons in the dimuon rest-frame, relative to the beam direction, is also $1+\cos^2\theta$ (see figure 6). Scaling in the variable $\tau = m_{\mu\mu}/\sqrt{s}$, where s is the square of the c.m. energy, also demonstrates point-like partons, as do figures 2 and 3.

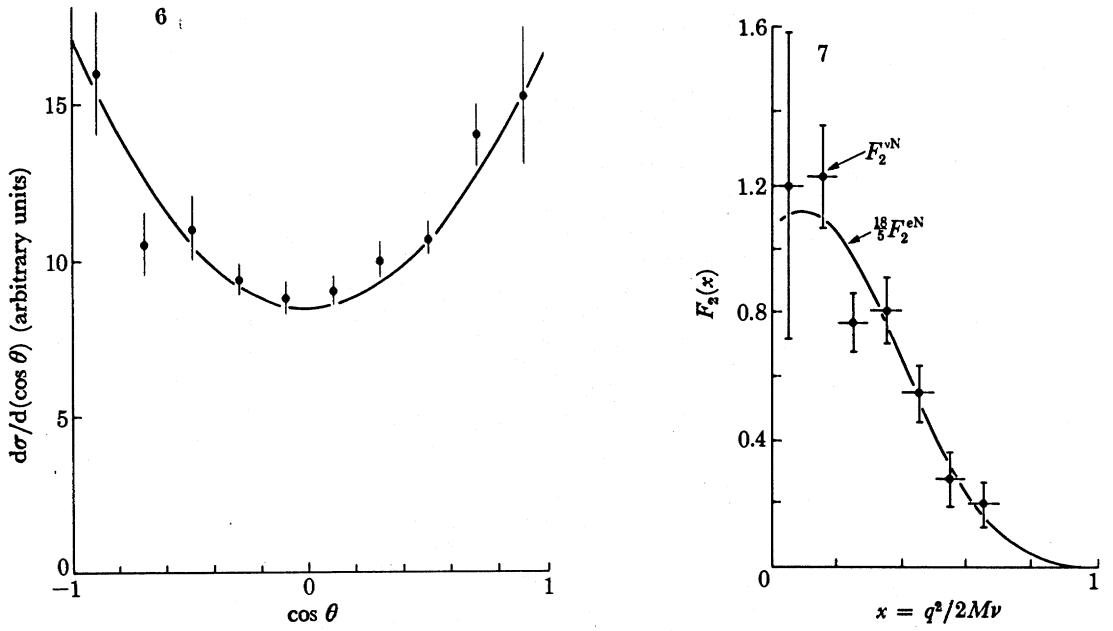

FIGURE 6. Angular distributions of Drell–Yan-produced muons, in the dimuon rest-frame, relative to the hadron beam direction (after Anderson *et al.* 1978). The solid line is the curve $1+\cos^2\theta$.

FIGURE 7. The data points show the Gargamelle PS results for $F_2^{\nu N}(x, q^2)$ $(q^2 > 1)$, and the solid line is the curve fitted through SLAC e–d data, giving $F_2^{eN}(x, q^2)$ $(q^2 > 1)$. The ratio is $\frac{5}{18}$, as expected for fractionally charged quarks.

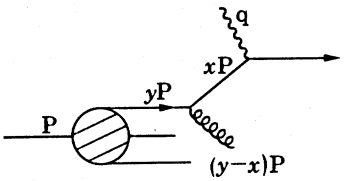

FIGURE 8.

The argument for partons having the fractional charges assigned to quarks comes from a straightforward comparison of $F_2^{eN}(x, q^2)$ with $F_2^{\nu N}(x, q^2)$, made in 1972. The ratio of these two quantities is just the mean square quark charge in a nucleon, $\frac{5}{18}$ (see figure 7).

3.2. *QCD predictions: the Altarelli–Parisi equations*

In leading order, QCD makes definite predictions for the behaviour of the structure functions in deep inelastic scattering. The simplest approach is via the Altarelli–Parisi (1977) equation for the non-singlet quark distribution in leading-order QCD:

$$\frac{\mathrm{d}\{Q_{NS}(x, q^2)\}}{\mathrm{d}\{\ln q^2\}} = \frac{\alpha_s(q^2)}{2\pi}\int_{y=x}^{y=1} P_{QQ}\left(\frac{x}{y}\right) Q_{NS}(y, q^2)\,\frac{\mathrm{d}y}{y}, \tag{4}$$

the derivation of which is self-evident from figure 8. As q^2 goes from low to high values, Q_{NS} can change only fractionally (since there is no scale) with q^2, which explains the form of the left-hand side. The logarithmic derivative depends on the splitting function

$$P_{QQ}(z) = \tfrac{4}{3}(1+z^2)/(1-z) \tag{5}$$

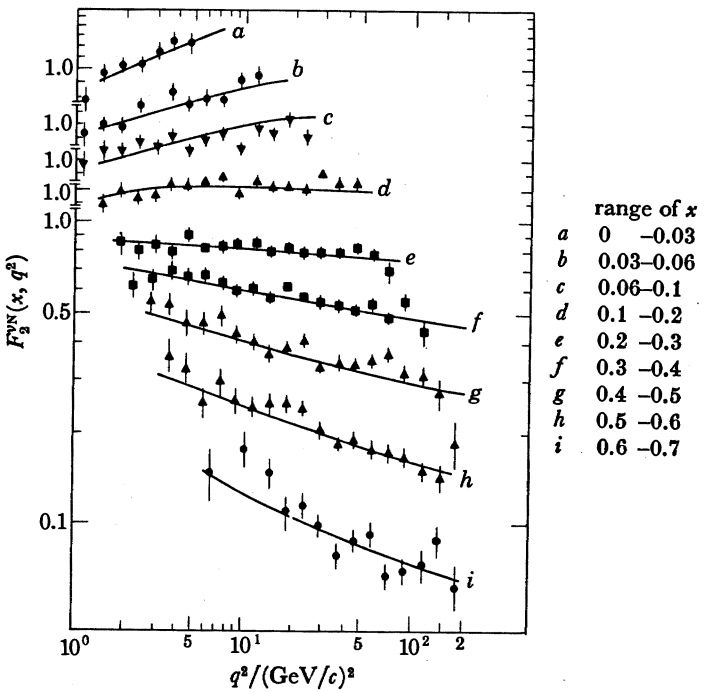

FIGURE 9. C.D.H.S. data of de Groot *et al.* (1979) on the q^2-dependence of structure functions $F_2^{\nu N}(x, q^2)$, measured in neutrino-scattering in iron.

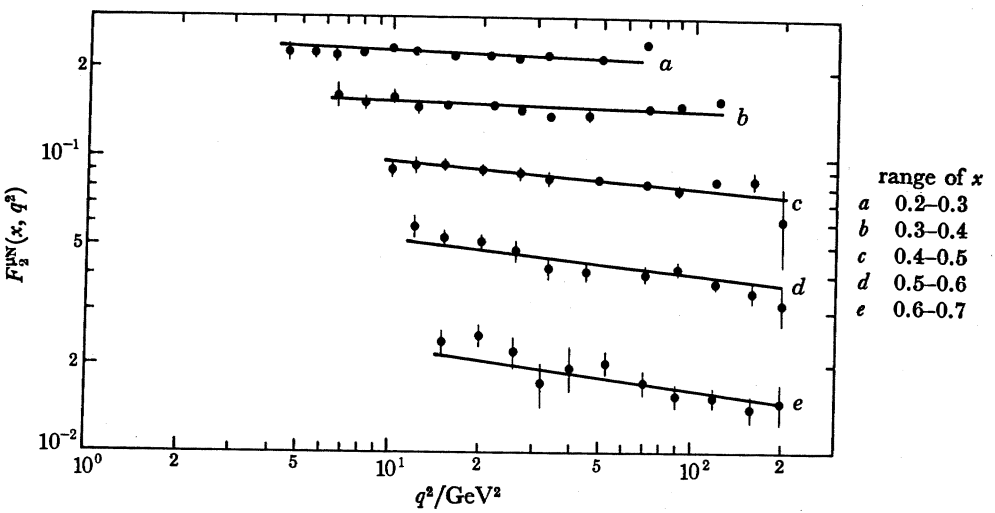

FIGURE 10. E.M.C. data of Aubert *et al.* (1980*a*) on the q^2-dependence of $F_2^{\mu N}(x, q^2)$, measured in muon-scattering in iron.

for finding a quark with momentum fraction z in a quark, as a result of bremsstrahlung, and on α_s, the probability of bremsstrahlung. The integral is for all values of $y > x$, since any quark can radiate a momentum fraction $y-x$ to attain a momentum fraction x. The most direct way to compare data with theory is to use (4) by evaluating the integral on the right-hand side numerically at fixed q^2 over the range $x < y < 1$, and then dividing it into the logarithmic derivative measured at fixed x over a small q^2-range. Note that data from $y = x$ to $y = 1$ are needed; however, because of the form of (5), the main contribution to the integral

of (4) is for y not too far from x. If there are no data at large x, even wild extrapolations are acceptable. The main problem is that the errors in the numbers on the left-hand side are large.

Applying this procedure to the combined structure function data of the C.D.H.S. collaboration (de Groot *et al.* 1979) measuring neutrino scattering in iron (see figure 9) and of the E.M.C. collaboration (Aubert *et al.* 1980*a*) measuring muon scattering in iron (see figure 10), I find no evidence for any q^2-dependence of α_s with q^2, about its mean value $\alpha_s \approx 0.2$, for the range $10 \leqslant q^2 \leqslant 150\ \mathrm{GeV}^2$. If one includes data down to $q^2 = 4\ \mathrm{GeV}^2$, there is a decrease of two standard deviations.

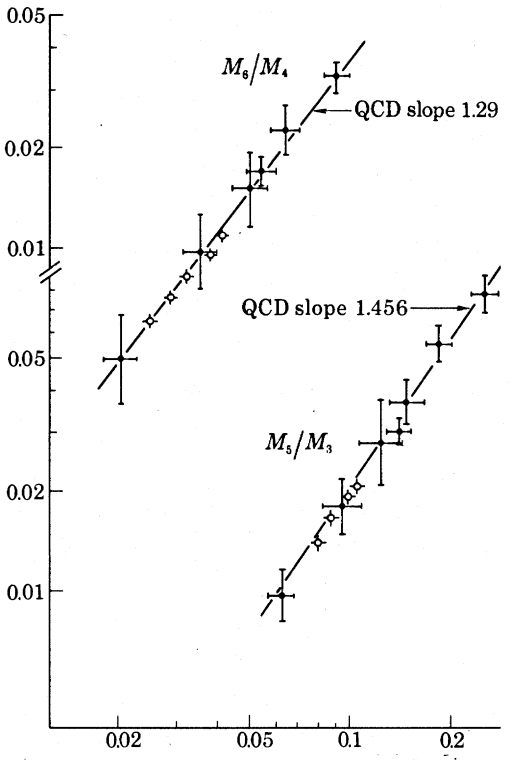

FIGURE 11. Logarithmic plots of B.E.B.C. (●) and C.D.H.S. (○) neutrino data from the Cern SPS. Comparison of the slopes is made with QCD predictions.

3.3. *Moments of structure functions*

If equation (4) is multiplied through by x^{N-1} and integrated from $x = 0$ to $x = 1$, the right-hand side factorizes and one obtains

$$\frac{\mathrm{d}\{M_{\mathrm{NS}}(N, q^2)\}}{\mathrm{d}\{\ln q^2\}} = \frac{\alpha_s(q^2)}{2\pi} A_N M_{\mathrm{NS}}(N, q^2), \tag{6}$$

where

$$M_{\mathrm{NS}}(N, q^2) = \int_0^1 x^{N-1} Q_{\mathrm{NS}}(x, q^2)\, \mathrm{d}x,$$

and

$$A_N = \int_0^1 z^{N-1} P_{\mathrm{QQ}}(z)\, \mathrm{d}z.$$

Equation (6) integrates to give, for the q^2-dependence of the moment,

$$M_{\mathrm{NS}} = \text{const.}/\ln\,(q^2/\Lambda^2)^{d_{\mathrm{NS}}}, \tag{7}$$

where

$$d_{\mathrm{NS}} = \frac{6A_N}{33-2f} = \frac{4}{33-2f}\left\{1 - \frac{2}{N(N+1)} + 4\sum_{j=2}^{N}\frac{1}{j}\right\} \tag{8}$$

and we have used for the strong coupling constant

$$\alpha_{\mathrm{s}}(q^2) = 12\pi/(33-2f)\ln(q^2/\Lambda^2), \tag{9}$$

f being the number of quark flavours. The prediction (7) is clear: the moments of the valence quark distribution functions vary as known powers of $\ln(q^2/\Lambda^2)$. Early experiments in B.E.B.C. at the SPS (Bosetti *et al.* 1978) could use the moment method as they measured over essentially the whole x-range. They found $\Lambda = 0.7$ GeV, or $\alpha_{\mathrm{s}}(q^2 = 10) = 0.46$ and $\alpha_{\mathrm{s}}(q^2 = 1) = 1.96$. Clearly one has to be doubtful about this result, since the leading-order QCD analysis presumes $\alpha_{\mathrm{s}}(q^2) \ll 1$. Strangely, the slopes of the logarithmic moment plots (giving the ratio of d_{NS} for different N-values) agreed with QCD (figure 11).

Much has been said about the pros and cons of the use of moments as against other methods. The only difference between the method with the use of (4) and that with the use of (7) is that for (4) one needs data only for $x = x$ to $x = 1$ while for (7) the whole range $x = 0$ to $x = 1$ is required. Of course, by selecting the value of N, the results from the moment method can be made to depend more or less on the data at small x or large x.

3.4. *Comparison with QCD by using structure functions directly*

Another method – and a necessary one for experiments with data over a limited range – has been to compare the structure functions directly with empirical fits to quark distributions. These are taken to be of the general form $x^{\alpha}(1-x)^{\beta}$ where α and β contain a q^2-dependence that gives moments agreeing (almost) with the QCD relation (7) (Buras & Gaemers 1978). The parameter Λ is one of several in the fit to the data. The C.D.H.S. (figure 9) and E.M.C. (figure 10) experiments have used this approach; they determine $\Lambda = 0.3$ GeV and $\Lambda \approx 0.1$ GeV respectively, for a similar q^2-range (10–150 GeV^2 approximately). The weakness of the method is that it *necessarily* involves assumptions about the form of $F_2(x, q^2)$ in regions where it is not measured (particularly $x > 0.7$). Another problem is that the values of Λ appear to disagree, indicating a q^2-dependence in the νN data, which is stronger than in the μN data, in the same regions of x and q^2.

3.5. *Higher-order corrections*

All the remarks above refer to Λ defined in (9) with α_{s} defined in leading order in (4). At low q^2, α_{s} is not small compared with unity, and higher-order $(\alpha_{\mathrm{s}}^2, \alpha_{\mathrm{s}}^3, \ldots)$ corrections are likely to be important. Many papers have been written about higher-order corrections (see for example, Bardeen *et al.* 1978, Floratos *et al.* 1977, 1978, 1979). The main effect of the inclusion of α_{s}^2-corrections is to reduce the value of Λ by about 50%, but hardly to affect the quality of the fits to the data. Higher-order corrections are important, but hardly crucial at this stage in attempting to test QCD.

3.6. *High twist effects*

The Altarelli–Parisi equation (4) treats the struck quark as if it were isolated from the other two, in inelastic lepton–nucleon scattering. There must be non-perturbative terms resulting from the effects of these 'spectators', involving extra factors in the q^2-dependence of the structure functions, of the general form $\{1 + f(x)\,M^2/q^2\}^r$, where $f(x)$ increases with x (for example,

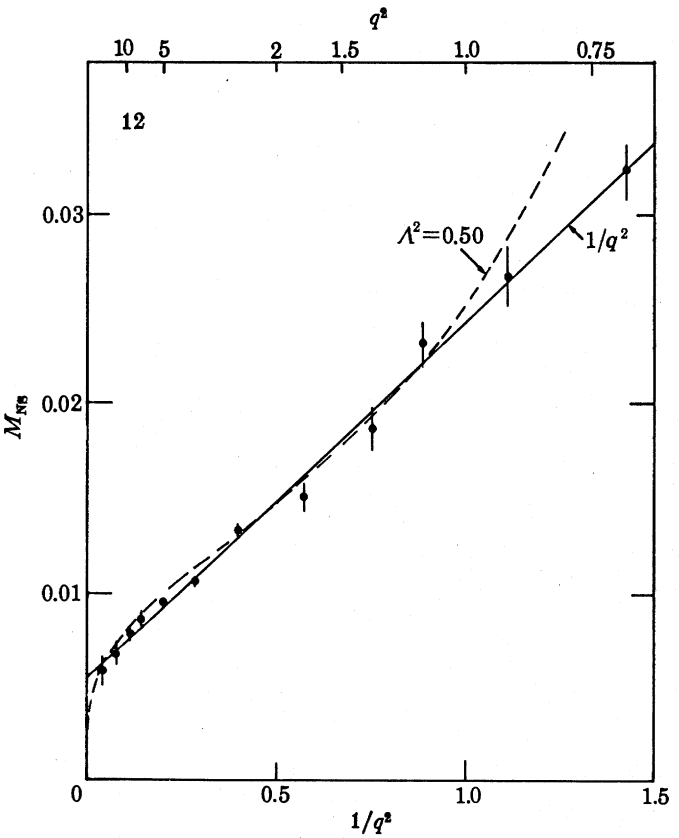

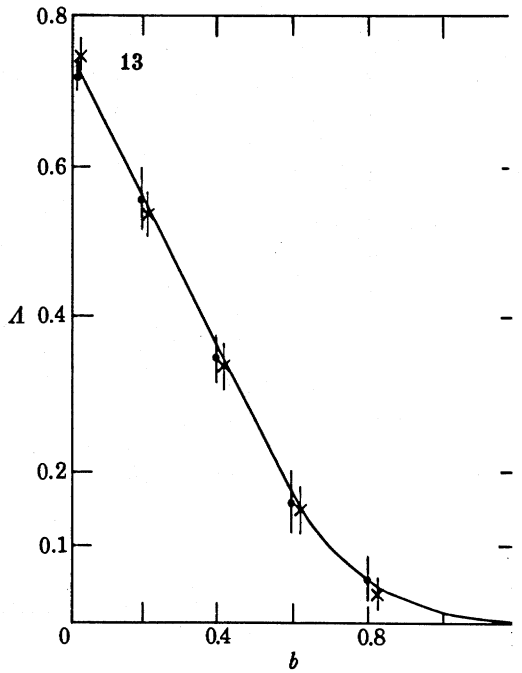

FIGURE 12. Analysis by the author of SLAC–CHIO data ($N = 4$). Both the QCD ($\ln q^2$) and high-twist ($A + B/q^2$)-dependences give a reasonable fit to the data.

FIGURE 13. Fits to SLAC–CHIO data on the non-singlet moments, with a combination of perturbative QCD and high-twist parametrizations, for $N = 3$ (●) and $N = 5$ (×) moments: M_{NS} is given by equation (10) below. The coefficient b and the value of Λ are almost completely correlated.

$f(x) \sim 1/(1-x)$), and where $r = 1, 2, \ldots$ corresponds to terms of twist 4, 6, ... We consider here only $r = 1$. The effect on the moments (7) is to multiply them by an additional factor, for example of the form $1 + \alpha NM^2/q^2$. The precise form of high-twist terms is however unknown, and an empirical approach is necessary. Such effects have been analysed by Abbott & Barnett (1979) for example. Figures 12 and 13 show an analysis by the author. Fits to moments can be made with a combination of the perturbative QCD form (7) and a high-twist term, i.e. of the form

$$M_{NS} = c\{1 + b(N - 1.5)/q^2\}/\ln (q^2/\Lambda^2)^{d_{NS}}, \qquad (10)$$

where Λ varies from 0.7 to 0 as b varies from 0 to 1 GeV^2. It is conceivable that, with much more accurate and detailed experiments, we might distinguish high-twist and perturbative effects, but the prospects are not good. The best way to avoid high twist effects is to do experiments where they are small (for example $e^+e^- \to$ hadrons), or at very large q^2, as at the proposed ep colliders (figure 14).

3.7. *The G.L.S. sum rule*

In this section on deep inelastic processes, I mention recent evaluations of the Gross–Llewellyn Smith sum rule (1969), made by the ABCLOS collaboration (figure 15). These

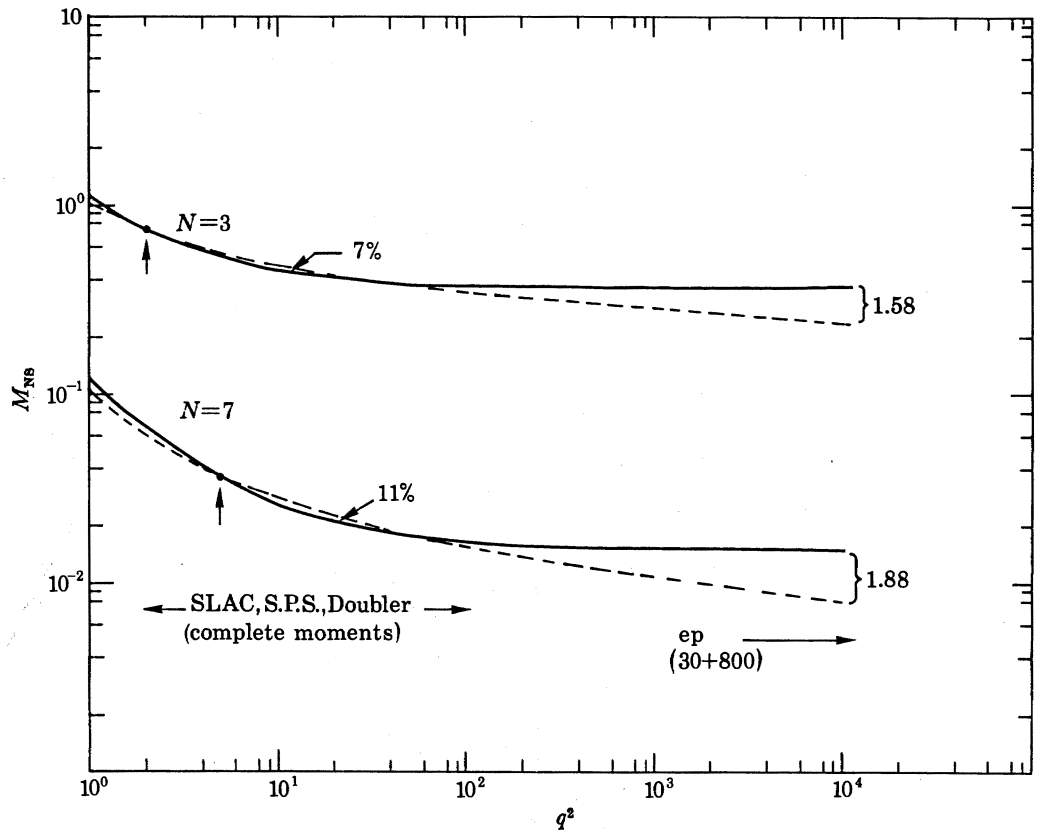

FIGURE 14. Variations of $N = 3$ and $N = 7$ moments with q^2 according to perturbative QCD (dashed line: $1/\{\ln(q^2/\Lambda^2)\}^{d_{NS}}$ with $\Lambda^2 = 0.40$) or to high-twist effects with parameters fitted to low-q^2 data (full line: $1+1.3(N-1.5)/q^2$). For $q^2 > 10^3$ GeV^2, the two effects are distinguishable.

are for the $N = 1$ Nachtmann moment of the non-singlet structure function F_3, where high twist effects should be small. The QCD prediction is very simple:

$$\int_0^1 F_3(x, q^2)\,\mathrm{d}x = 3\left\{1 - \frac{\alpha_s(q^2)}{\pi}\right\}. \tag{11}$$

The data show that the integral is nearly constant, from $q^2 = 10$ GeV^2 (the safe upper limit above which corrections, depending on the precise form of $F_3(x)$ at very small x, may be required) down to $q^2 = 0.1$ GeV^2. At the lowest q^2, the cross section is dominated by elastic and resonance (Δ) processes. Although the interpretation of the results is not straightforward at very low q^2, the results do suggest a value for $\Lambda < 0.3$ GeV.

3.8. *Abelian nature of QCD*

There is little evidence for the gluon–gluon coupling from deep inelastic scattering. Figure 16 shows one result, on the integral of $F_2(x, q^2)$ from $x = 0$ to $x = 1$, from SLAC data and from neutrino bubble chamber experiments at Cern. For $2 \leqslant q^2 \leqslant 20$ GeV^2, the integral appears to decrease, and according to Glück & Reya (1979) this is evidence for non-Abelian coupling. Other field theories (fixed-point, non-asymptotically-free) would predict the quark momentum fraction *increasing* with q^2. Because of high-twist terms of unknown magnitude, however, it is hard to reach any firm conclusion.

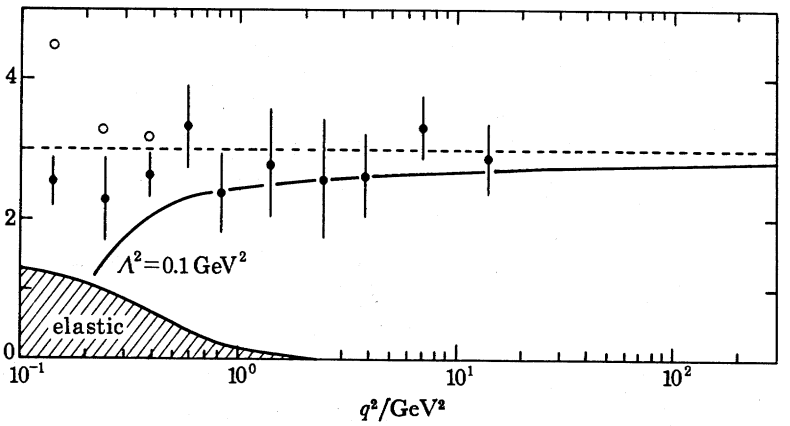

FIGURE 15. The evaluation of the G.L.S. sum rule from Gargamelle and B.E.B.C. experiments. ●, $N = 1$, Nachtmann moment of xF_3; ○, $N = 1$, Cornwall–Norton moment of xF_3; – – –, Parton model prediction; ——, QCD prediction $3(1-\alpha_s/\pi)$.

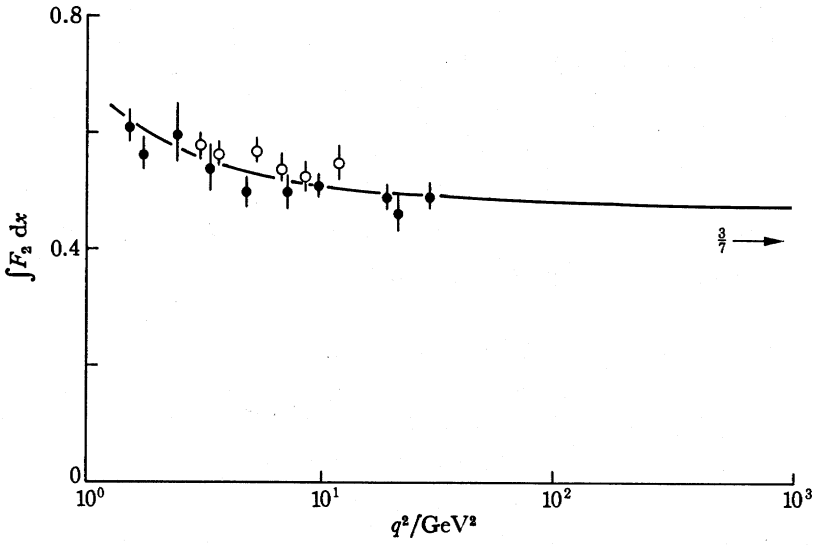

FIGURE 16. $\int_0^1 F_2(x, q^2)\,dx$ from νN data in B.E.B.C. and Gargamelle, and from SLAC ed scattering. The curve shows the prediction from QCD for $\Lambda \approx 0.5$. If non-perturbative (high-twist) terms could be excluded, the decrease of the integral with q^2 would be definite evidence for an asymptotically free, non-Abelian gauge theory (QCD), as pointed out by Glück & Reya (1979).

4. TESTS OF QCD IN HADRONIC FINAL STATES IN LEPTOPRODUCTION AND e^+e^- ANNIHILATION

The other major area in which QCD predictions have been tested is in the study of hadronic final states in lepton–nucleon scattering, and e^+e^- annihilation to hadrons.

Much work has been done, mostly with neutrino reactions in bubble chambers, on the q^2-evolution of the distribution in fractional energy, z, carried by individual hadrons (the so-called fragmentation functions). In particular, the non-singlet distributions (h^+–h^-) fit the QCD predictions quite well (figure 17). However, the q^2-range is low so that non-perturbative effects may be important.

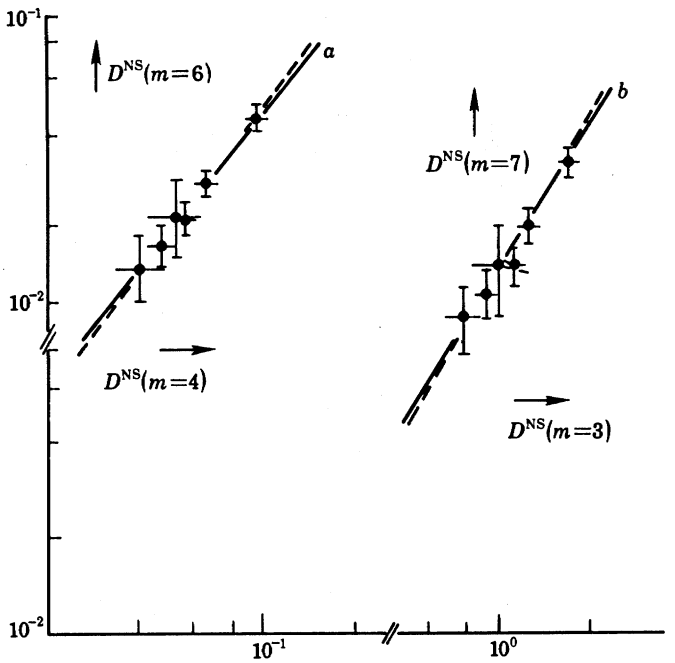

FIGURE 17. Moments of non-singlet fragmentation functions measured by the ABCMO collaboration in the B.E.B.C. chamber (Blietschau *et al.* 1979). The slopes in these plots are compatible with QCD predictions: *a*, slope 1.27 ± 0.10, QCD slope 1.29; (*b*), slope 1.67 ± 0.17, QCD slope 1.76.

I shall therefore limit the discussion to transverse hadron distributions, on which there is a considerable range of data from a variety of experiments.

4.1. *W-dependence of p_T distributions*

One of the characteristic features of hadron final states in μN and νN scattering and in e^+e^- annihilation is the broadening of the distribution of p_T of individual hadrons relative to the resultant momentum vector of all the hadrons, as W increases. Figure 18 shows νN and μN data on hadrons in the forward direction in the overall hadron c.m. system, where p_T is measured for each hadron relative to the q vector, and $\overline{p_T^2}$ is the value averaged over all forward hadrons. One observes a slow increase of $\overline{p_T^2}$ with W^2. At low W, some of this must be of purely kinematic origin (the so-called 'seagull effect') owing to the fact that $p_T(\max) < \frac{1}{2}W$, and so secondaries in the high-p_T 'tail' are absent. However, phase-space calculations (as well as common sense) show that this cannot be the explanation for the increase for $W > 10$ GeV. Hadronization of the quarks is concerned with interactions over a volume of dimensions *ca.* R_0^{-1} where R_0 is the r.m.s. radius of a hadron. So, values of $\overline{p_T^2} \gg R_0^{-2} \approx 0.1$ GeV^2 *must* correspond to some other phenomenon.

Having myself introduced, over 20 years ago (Edwards *et al.* 1958), the term 'jet' in cosmic ray studies and first shown that in hadron–hadron collisions $\overline{p_T}$ is limited to a value of *ca.* 0.3 GeV/c, almost independent of energy, from a few gigaelectronvolts to *ca.* 10^6 GeV, I feel a responsibility to stress this point. Large values of p_T in lepton–quark interactions *must* originate from hard scattering processes which will, just from dimensional arguments, lead to $\overline{p_T^2} \propto W^2$, when W is large compared with a typical hadron mass, $M \approx M_p$.

One source of large-p_T processes is the bremsstrahlung of one or more gluons by the acce-

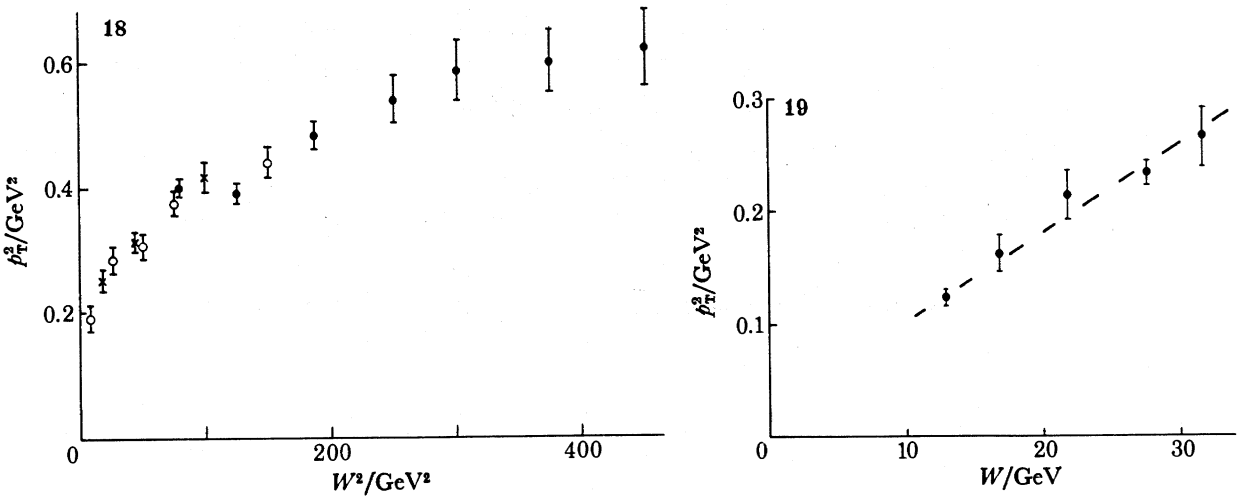

FIGURE 18. Data for p_T^2 of forward hadrons produced in neutrino–nucleon scattering (Allen *et al.* 1980) and in muon–nucleon scattering (Aubert *et al.* 1980*b*). ×, ○: B.E.B.C. νH_2, νNe, experiments, made by the ABCMO collaboration. ●, E.M.C. μH_2 experiments.

FIGURE 19. Data for p_T^2 of hadrons produced in e^+e^- annihilation, as a function of W. The p_T of each hadron is measured relative to the sphericity axis (defined in the text) (Brandelik *et al.* 1979).

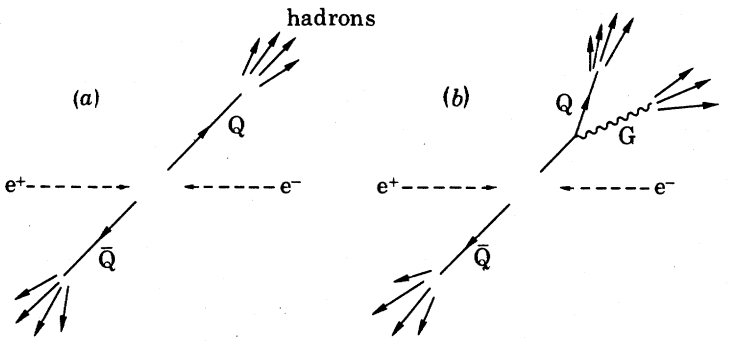

FIGURE 20. Diagram illustrating single hard gluon bremsstrahlung by one of the quarks in e^+e^- annihilation, leading to a 'three-jet' event (see also figure 23).

lerated quark, as for example in figure 20. In lepton–nucleon scattering, the contributions to p_T are often written in the form

$$[\overline{p_T(z)}]^2_{had} = (\overline{p_T^2})_{frag} + z^2[\overline{k_T^2} + (\overline{p_T^2})_{QCD}], \tag{12}$$

where in leading order, i.e. on the assumption of *single* gluon bremsstrahlung,

$$\begin{aligned}(\overline{p_T^2})_{QCD} &= \alpha_s(q^2)\, q^2 f(x, y)\\ &= \alpha_s(q^2)\, kW^2,\end{aligned} \tag{13}$$

where, from the kinematics of quark–gluon scattering, it is easy to show the (q^2, x)-dependence takes the form $q^2(1/x - 1) \approx W^2$. The constant k depends on fragmentation functions, but is typically 0.04. The quantity k_T is the primordial transverse momentum of a quark in a nucleon and $(\overline{p_T^2})_{frag}$ is the (constant) contribution from hadronization of quarks or gluons. It is not known if it is really possible to separate the terms as in (12). If it is, one can fit the data in

figure 18 to find $\overline{k_T^2}$ and α_s. A check is possible since $\overline{k_T^2}$ can be found independently by separating forward and backward hadrons in 3C fit events where all hadrons are detected. Both methods give $\overline{k_T^2} \approx 0.4$ GeV^2. So, α_s can be deduced from the lepton data; its value turns out to be rather large ($\alpha_s \approx 0.5$). There is, however, other evidence that (12) taken in conjunction with (13) is incorrect in the (W^2, q^2)-regions investigated to date. This is discussed below.

The increase in $\overline{p_T^2}$ with W^2 is observed also in e^+e^- annihilation to hadrons, as shown in figure 19. The smaller values of $\overline{p_T^2}$ in this process – as compared with lepton scattering – arise from the fact that in e^+e^--annihilation, p_T is minimized, by definition of the sphericity axis with respect to which it is measured.

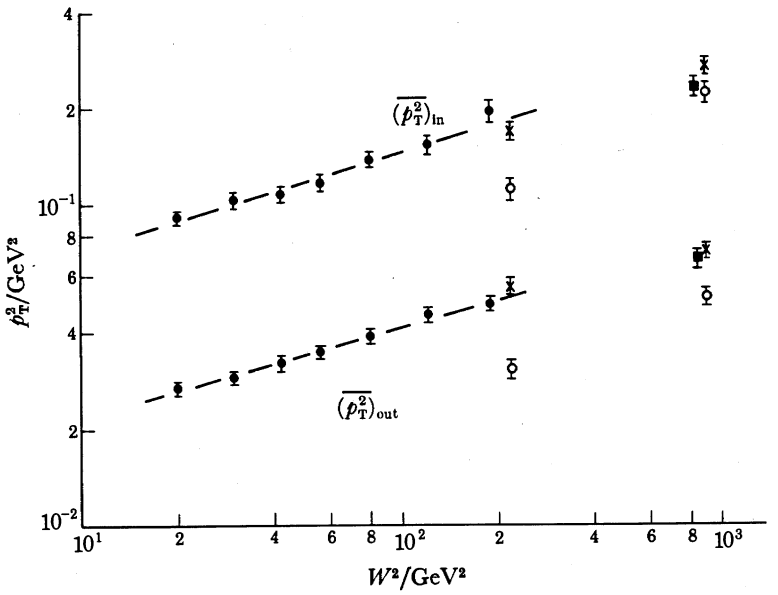

FIGURE 21. Components $(\overline{p_T^2})_{in}$ and $(\overline{p_T^2})_{out}$ of hadrons relative to the event plane. In the neutrino data (●), this is defined as the plane containing the q-vector that minimizes Σp_T^2 measured relative to q and perpendicular to the plane. In e^+e^- reactions (⊖, TASSO), the plane is the Q_2–Q_3 plane where Q_3 and Q_2 are the largest and next-largest of the three eigenvalues defined in (15). Because of the different definitions, the absolute values from e^+e^- and νN reactions differ. Both $(\overline{p_T^2})_{in}$ and $(\overline{p_T^2})_{out}$ show about the same fractional increase with W^2, in both sets of data. ⧳, νN data; e^+e^- data: ⊖, TASSO; ⧲, PLUTO; ⧳, JADE.

4.2. *Planar events:* $(\overline{p_T^2})_{in}$ *and* $(\overline{p_T^2})_{out}$

If *single* hard gluon bremsstrahlung by the struck quark (or, in e^+e^- collisions, the produced quark or antiquark) is a dominant process, the hadrons will tend to lie in a plane (close to the quark–gluon scattering plane, as in figure 20). Analyses have therefore been done to determine the hadron plane. In e^+e^- events, this is done by a minimization procedure: the eigenvalues Λ_1, Λ_2, Λ_3 of the momentum ellipsoid of each event are found by diagonalizing the 3×3 matrix

$$M_{\alpha\beta} = \sum_{j=1}^{N} P_{j\alpha} P_{j\beta}, \tag{14}$$

where α, β are x, y or z, and the sum extends over all N secondaries of the event. The normalized eigenvalues

$$Q_{1,2,3} = \Lambda_{1,2,3}/\Sigma P_j^2, \tag{15}$$

are such that $Q_1+Q_2+Q_3 = 1$, and they are defined in the order $Q_3 > Q_2 > Q_1$. Thus Q_3 defines the longest axis (the sphericity axis which minimizes the transverse momentum components), and Q_2, Q_1 define the transverse axes. The quantity $(\overline{p_T^2})_{in}$ is the mean-square component in the (Q_2, Q_3)-plane, and $(\overline{p_T^2})_{out}$ is that normal to it, where by definition $(p_T^2)_{in} > (p_T^2)_{out}$. The sphericity and aplanarity are defined as

$$S = \tfrac{3}{2}(Q_1+Q_2) = \tfrac{3}{2}(1-Q_3) = \tfrac{3}{2}\min \Sigma p_{Tj}^2/\Sigma p_j^2, \qquad (16)$$
$$A = \tfrac{3}{2}Q_1.$$

In lepton–nucleon scattering, the axis Q_3 is taken as that of the q-vector (the resultant hadron momentum vector, corrections being made for missing hadrons), and only the eigenvalues Q_2 and Q_1 are required to define the hadron plane. Figure 21 shows the results from both sets of experiments. In the νN data, the values are for forward hadrons only, in events with at least three forward hadrons. In both this and the e^+e^- data, both $(\overline{p_T^2})_{in}$ and $(\overline{p_T^2})_{out}$ grow with W^2 at about the *same fractional rate*. This means that most of the events have a secondary distribution *azimuthally symmetric* about the event (q or Q_3) axis. So most of the p_T^2 increase with W^2 is *not* due to single hard gluon bremsstrahlung. It can however be understood if several hard scattering processes take place off the accelerated quark, rather as in multiple coulomb scattering.

I have not shown the μN (E.M.C.) data in figure 21. The E.M.C. collaboration do not give $(\overline{p_T^2})_{out}$ and $(\overline{p_T^2})_{in}$ as a function of W^2. Their average ratio of these two quantities is *ca.* 8, compared with *ca.* 4 in νN and e^+e^- data. The ratio clearly will depend on multiplicity (it is infinite for multiplicity 2!) and selection biases, which are likely to be much more serious in μN scattering than in the essentially '4π' detectors like B.E.B.C. or at PETRA.

4.3. *Planar events: selection of 'three-jet' candidates*

While most hadrons in most events are therefore created with azimuthal symmetry about the jet axis, one can ask if a subsample of events are in some way special (for example corresponding to *single* hard gluon bremsstrahlung). In exactly the same way, in the process of scattering of a charged particle traversing an absorber, the Rutherford (single) scattering 'tail' can be found, at large scattering angle, projecting clear of the multiple scattering distribution. Effectively all methods rely on selecting events with secondaries of anomalously large p_T, in the hope that some of them will correspond to the perturbative QCD leading-order process of single hard scattering via gluon emission at wide angle by the quark.

In the e^+e^- experiments, selections were made on the S- and A-values in (16). Large S means one or more secondaries have very large p_T, and small A implies $(p_T^2)_{in} \gg (p_T^2)_{out}$ in that event. For example, in the TASSO analysis (Brandelik *et al.* 1979), the following numbers of events were found in different regions of S and A.

selection	observed	$Q\bar{Q}$ M.C.	$Q\bar{Q}G$ M.C.
$S > 0.25$; $A < 0.04$	18	4.5	17
$S > 0.25$; $A > 0.04$	38	38	35

The distributions in A and S are shown in figure 22.

The observed numbers agree much better with the Monte-Carlo (M.C.) generating hadrons according to the $Q\bar{Q}G$ process (as in figure 20) than with the 'two-jet' Monte Carlo, $Q\bar{Q}$.

The other PETRA groups (PLUTO, JADE, MARK J) found similar results. Figure 23 shows an example of a 'three-jet' candidate. From the rate of these events, it is possible to estimate α_s, and to determine the ratio of 'three jet' to 'two-jet 'events. All four groups find about the same value:

$$\alpha_s(e^+e^- \to \text{hadrons}\ (W \approx 30\ \text{GeV})) = 0.18 \pm 0.05. \qquad (17)$$

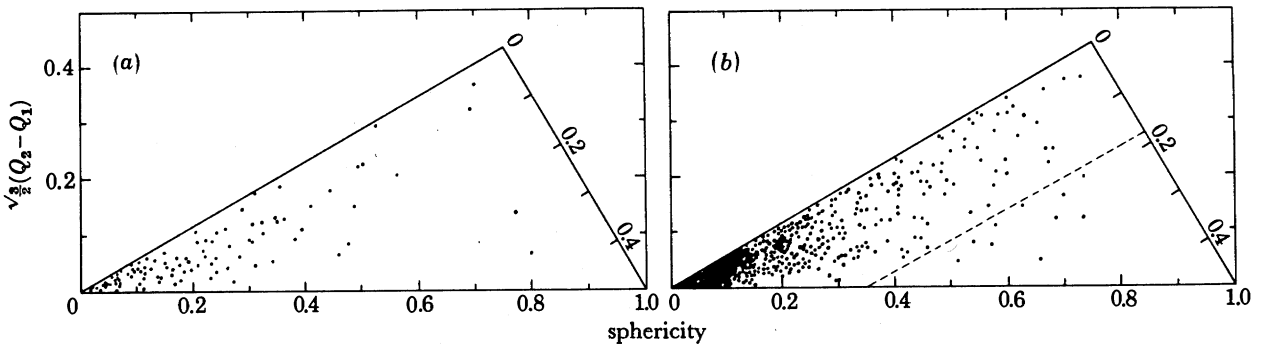

FIGURE 22. Dalitz plot of the eigenvalues Q_1, Q_2, Q_3 of equation (15) in the TASSO experiment: (*a*) $13 \leqslant W \leqslant 17$ GeV; (*b*) $29.9 \leqslant W \leqslant 31.6$ GeV. Near the upper side of the triangle are the so-called planar events of $S > 0.25$ and $A < 0.04$. The increase in the proportion of these in the higher W-range is apparent. (Brandelik *et al.* 1979).

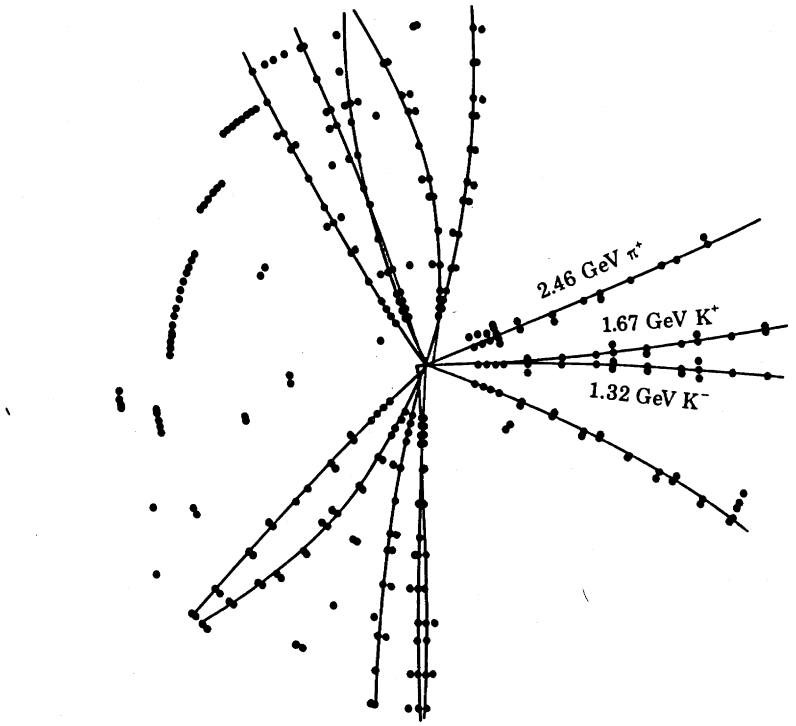

FIGURE 23. Candidate three-jet event in TASSO experiment, ascribed to hard gluon bremsstrahlung by one of the quarks in the process $e^+e^- \to Q\bar{Q}$, $Q \to Q+G$; $E_{c.m.} = 35$ GeV, $M_{K^+K^-} = 1.01$ GeV, $\phi \to K^+K^-$.

There is some doubt about the value of q^2 to which this corresponds. Is q^2 equal to W^2, the invariant mass of quark and gluon jets, etc.? So q^2 is somewhere in the range 300–1000 GeV^2. For five quark flavours, (9) then gives $\Lambda = 0.25(\pm 0.25)$ GeV. The PETRA groups have also

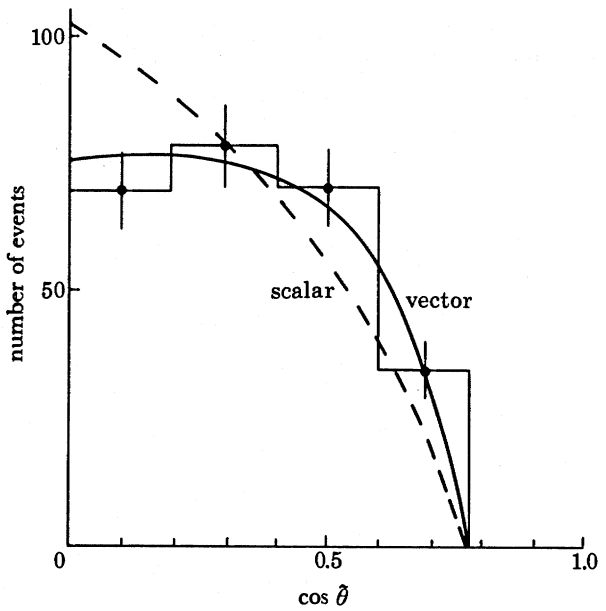

FIGURE 24. Distribution in angle $\tilde{\theta}$ between the momentum vector of the quark assigned to the 'slim jet', and the common line of flight of quark and gluon producing the 'fat jet', measured in the QG c.m.s. system, in 'planar three-jet' events (Brandelik *et al.* 1980).

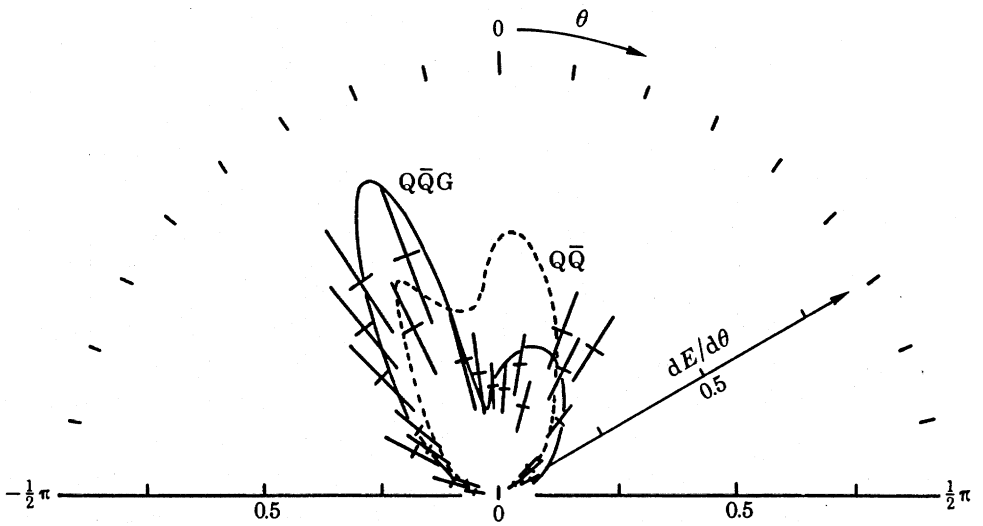

FIGURE 25. Polar angle distribution of energy flow relative to the q-vector in μp events with $10 \leqslant W \leqslant 20$ GeV, more than three charged hadrons forward, and at least one charged hadron with $p_T > 1.5$ GeV/c. The data show a forward two-lobe structure which is in better agreement with the QQ̄G Monte Carlo program than the QQ̄ Monte Carlo program. (Aubert *et al.* 1981).

investigated the gluon spin by exploiting the fact that, in the process $e^+e^- \to \bar{Q}+Q, G$, the angle $\tilde{\theta}$ between the $\bar{Q}$-direction and the common line of flight of Q and G, in their c.m. system, depends on the scalar or vector character of the gluon. The data (figure 24) favour vector gluons.

In the lepton–nucleon scattering experiments, different analyses have been made. In the muon (E.M.C.) experiments, 'planar' events have been selected by requiring at least one forward hadron of $p_T > 1.5$ GeV/c, and for such events, the polar angle distribution of energy

flow of the forward hadrons $dE/d\theta$, relative to the q-vector, is plotted (figure 25). The double-lobe structure necessarily follows from the selection of a high-p_T secondary, from momentum conservation. The claim, however, is that the observed structure follows the $Q\bar{Q}G$ prediction better than $Q\bar{Q}$. The events are in the W-range 10–20 GeV.

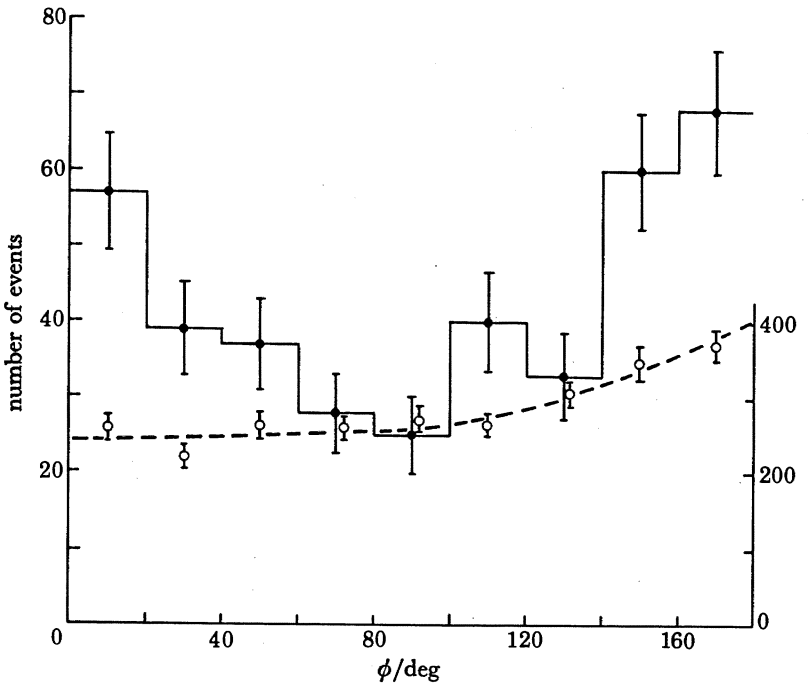

FIGURE 26. Azimuthal distribution of forward secondaries in events for $W > 10$ GeV ($q^2 > 1$ GeV, $x_F > 0$), relative to the secondary of highest p_T (called p_T^{max}). With no restriction on p_T^{max} (○, 677 events), the distribution is fairly flat; the peak towards $\phi = 180°$ is from momentum conservation. For $p_T^{max} > 1$ GeV/c (●, 95 events), however, there is a pronounced peak towards $\phi = 180°$ *and* one near $\phi = 0°$; some secondaries 'follow' the peak of highest p_T (unpublished data from B.E.B.C νNe and νH_2 experiments.)

The neutrino data (indicated in figure 26) are at lower W (10–15 GeV). Planar events are selected according to the criterion of four or more forward particles, of which at least one should have $p_T > 1$ GeV/c. The plot is the azimuthal distribution of forward secondaries relative to that at highest p_T (which is *not* included – as it is in figure 25). If no restriction is made on the value of the p_T of the secondary of largest p_T, the distribution is rather flat, with a bias to 180°, from momentum conservation. For $p_T^{max} > 1$ GeV/c, however, the 180° peak is more pronounced, but some particles *follow* the highest p_T particle – again a 'two-forward-jet' effect. This last analysis, incidentally, is the only one that does not depend on comparison with a Monte-Carlo program.

It has to be said that both leptoproduction experiments are at lower W than the e^+e^- experiments, and the proportion of '$Q\bar{Q}G$' events is very small (*ca.* 2–3% of the total) contrasting with *ca.* 15% in e^+e^- annihilation at $W \approx 30$ GeV. The e^+e^- data therefore provide more convincing evidence than that from leptoproduction.

Conclusions

Our general conclusion is that, in the study of deep-inelastic scattering and e^+e^- annihilation processes, QCD has been subject to some qualitative tests. The structure functions do show a q^2-dependence of the type expected, but unexplained discrepancies between experiments prevent any sharper conclusions. Structure function analysis is beset with the problem of high-twist contributions, and thereto hangs a major problem. The high-q^2 data, and the G.L.S. sum rule result suggest $\Lambda \approx 0.1$ GeV only. The low q^2-data then suggest twist-4 coefficients (the quantity b in (10)) of order 0.7–1 GeV^2. Naively, we would expect Λ^2 and b to be of the same order, since they are determined by some characteristic hadron mass scale. Why then is the high twist coefficient so large and Λ so small?

In hadron final states, the broadening of the p_T-distribution as W increases, in deep inelastic processes and in e^+e^- annihilation, is indicative of point-like hard scattering processes, as predicted by QCD. There is indeed evidence, principally from the e^+e^- data, that a small proportion of events can be attributed to *single* hard gluon bremsstrahlung at wide angle, by one of the quarks. This evidence depends on a comparison between the data and the predictions of Monte-Carlo programs incorporating hadronization, for the processes $e^+e^- \to Q\bar{Q}$ and $e^+e^- \to Q\bar{Q}G$, and the latter gives a much better account of the 'planar' events. Although calculations exist also for the process $e^+e^- \to Q\bar{Q}GG$, they have not been confronted seriously with the data, so the claim that the PETRA planar events correspond to $Q\bar{Q}G$ *and nothing else* still has to be substantiated.

Quantitative tests of QCD, of the sort that have been made for QED, are still missing. We do not know if α_s really decreases logarithmically with q^2, or even that it decreases at all. Nor is there any convincing evidence for the non-Abelian character of the theory, that is the existence of gluon self-coupling. On the other hand, it does account qualitatively or semi-quantitatively for an enormous range of data, of which only a small part has been discussed here.

References (Perkins)

Abbot, L. F. & Barnett, R. M. 1979 SLAC-PUB 2325.

Altarelli, G. & Parisi, G. 1977 *Nucl. Phys.* B **126**, 298.

Allen, P. *et al.* (ABCMO collaboration) 1980 In *Proc. Neutrino* '80 *Conf.*, Erice, Sicily (ed. E. Fiorini). New York: Plenum Press.

Anderson, K. J. *et al.* 1978 In *19th Int. Conf. on High Energy Physics*, Tokyo. Tokyo: Physical Society of Japan.

Aubert, J. J. *et al.* 1980*a* *Physics Lett.* B **95**, 306.

Aubert, J. J. *et al.* 1980*b* *Proc. 20th Int. Conf. on High Energy Physics*, Madison, Wisconsin (ed. L. Durand & L. G. Pondrom). New York: American Institute of Physics.

Aubert, J. J. *et al.* 1981 Reprint CERN EP/81–10.

Bardeen, W. A. *et al.* 1978 *Phys. Rev.* D **18**, 3998.

Blietschau, J. *et al.* 1979 *Physics Lett.* B **87**, 281.

Bosetti, P. C. *et al.* 1978 *Nucl. Phys.* B **142**, 1.

Brandelik, R. *et al.* 1979 *Physics Lett.* B **86**, 243.

Brandelik, R. *et al.* 1980 Preprint DESY 80/80.

Buras, A. J. & Gaemers, K. J. 1978 *Nucl. Phys.* B **132**, 249.

Callan, C. G. & Gross, D. G. 1969 *Phys. Rev. Lett.* **22**, 156.

Edwards, B. *et al.* 1958 *Phil. Mag.* **3**, 237.

Floratos, E. G. *et al.* 1977 *Nucl. Phys.* B **129**, 66.

Floratos, E. G. *et al.* 1978 *Nucl. Phys.* B **139**, 545.

Floratos, E. G. *et al.* 1979 *Physics Lett.* B **80**, 269.

Glück, M. & Reya, E. 1979 *Nucl. Phys.* B **156**, 456.

de Groot, J. G. H. *et al.* 1979 *Phys.* C **1**, 143.

Gross, D. J. & Llewellyn-Smith, C. H. 1969 *Nucl. Phys.* B **14**, 337.

Riordan, E. M. *et al.* 1975 SLAC-PUB 1634.

Wiik, B. H. 1980 Report DESY 80/124.

PHILOSOPHICAL TRANSACTIONS OF THE ROYAL SOCIETY A MATHEMATICAL, PHYSICAL & ENGINEERING SCIENCES